# Highly Conducting and Flexible Few-Walled Carbon Nanotube Thin Film

Nanjundan Ashok Kumar,[†,§] In-Yup Jeon,[†,§] Gyung-Joo Sohn,[†] Rahul Jain,[‡] Satish Kumar,[‡] and Jong-Beom Baek[†,*]

[†]Interdisciplinary School of Green Energy/Institute of Advanced Materials & Devices, Ulsan National Institute of Science and Technology (UNIST), 100, Banyeon, Ulsan 689-798, South Korea, and [‡]School of Materials Science and Engineering, Georgia Institute of Technology, 801 Ferst Street, Atlanta, Georgia 30332-0295, United States. [§] These authors contributed equally to this work.

The tremendous and rapid growth witnessed recently in the area of nanosciences and nanotechnology as well as its recent exploration in various other research fields makes carbon nanotubes (CNTs) alluring.[1−4] Especially, the exotic properties such as high mechanical strength, flexibility, and impressive electric conductivity make it the most attractive and ultimate candidate for several applications, which include nanodevices, organic electronics,[5−8] and even transparent conductive films.[9,10]

Recently, few-walled carbon nanotubes (FWNTs), defined as nanotubes with sidewalls typically of 2 to 6 layers, diameters ranging from 3 to 8 nm, and lengths around tens of micrometers, have particularly distinguished them from other types of CNTs.[11] They tend to display the appropriate combination of their remarkable electronic properties and near perfect graphitization structures, which indicate their potential in field emission and nanocomposite applications.[12] The ability to chemically functionalize FWNTs with conducting matrices to generate nanocomposite hybrid materials or even thin films has stimulated much research interest not only for its easiness in synthesis and purification[13] but also for its high structural perfection and, particularly, good tolerance to surface functionalization procedures.[14] This is an especially attractive target because FWNTs can keep the structural integrity of their inner tubes after functionalization, and hence, the generated compounds are more compatible with composites and more dispersible in hosts, ultimately paving the way for important applications of FWNT-based composites. Recent studies have demonstrated that such a material is the best compromise as structural reinforcing fillers and in polymer composites.[11]

**ABSTRACT** We report an effective route to prepare highly conducting and flexible few-walled carbon nanotube (FWNT) thin films. The free-standing thin films were fabricated by functionalizing FWNTs with 4-ethoxybenzoic acid (EBA) *via* a direct Friedel−Crafts acylation reaction in a nondestructive polyphosphoric acid/phosphorus pentoxide medium. The resulting ethoxybenzoyl-functionalized FWNT (EBA-*f*-FWNT) was readily dispersible in water. EBA-*f*-FWNT thin films were formed by a simple suction filtration of the dispersed solution. Electron microscopic studies were employed to characterize the morphologies of the resulting thin films. The obtained results indicate that the structure of FWNTs was not perturbed by the incorporation of EBA moieties, which were uniformly grafted onto FWNTs forming the FWNT networks. Room temperature electrical conductivity of the thin films was obtained using standard four-probe measurements, which revealed a value as high as 29 400 S m$^{-1}$, while the tensile strength and modulus of the film were found to be about 80 MPa and 15 GPa, respectively. Cyclic voltammograms revealed a rectangular shape, with superior capacitive behaviors nearing 133 F/g for the thin films, which is very attractive for capacitor applications.

**KEYWORDS:** few-walled carbon nanotubes · functionalization · conducting thin film · mechanical properties · electrochemistry

Various methods for enhancing the interaction between CNTs and polymers were adopted in the recent past which included two main routes, namely, covalent sidewall grafting (linkage) and noncovalent adsorption or exohederal interactions, which provided access to such composites.[15−18] While both methods had their own merits depending on the platform, the traditional covalent functionalization strategy of the CNT is most frequently initiated by chemical acid oxidation acid treatment. However, dramatic amounts of induced defects during functionalization hinder the intrinsic mobility of carriers along CNTs, which is not preferred in any case. This method not only functionalizes the nanotube surfaces with carboxylic acid groups but also leaves behind detrimental structures, hence hampering their potential for practical

applications. Therefore, as a common rule, a now widespread approach to alleviate these problems is to find alternative routes such as an effective functionalization method that can not only introduce high density and homogeneous surface functional groups, which enhance the compatibility between CNTs and the foreign matrix, but also allow direct grafting and have little or no structural damage to the CNTs, thus, optimizing their properties for various applications.

To overcome this challenge, we have developed an efficient route to covalently functionalize CNTs *via* direct Friedel−Crafts acylation technique.[19−21] Considerable achievements have been made in enhancing the various functionalities of CNT−polymer nanocomposites, generally not achievable for each of the components individually.

Given the importance of such composite thin films, in this work, free-standing thin films composed of FWNT hybrids were successfully prepared starting from 4-ethoxybenzoic acid (EBA). Our strategy involves the covalent functionalization of EBA to FWNTs *via* a direct Friedel−Crafts acylation reaction in a polyphosphoric acid (PPA)/phosphorus pentoxide ($P_2O_5$) medium. The resulting EBA-*f*-FWNT was dispersible in water, and thus, EBA-*f*-FWNT thin films were fabricated by a simple suction filtration. The formations of the thin film heterostructures and their mechanical and electrochemical properties were characterized by necessary analytical techniques, and the results are delineated in the forthcoming sections.

## RESULTS AND DISCUSSION

Surface functionalization of CNTs is a frequently used method for covalently attaching foreign moieties to the surface of tubes. This strategy is considered as one of the versatile ways to produce coatings on any given surface. On the whole, surface functionalization not only enhances the reactivity but also improves the specificity and provides an avenue for further chemical modification of CNTs. However, care should be taken as extreme chemical oxidation treatments can compromise the properties of the resulting hybrids prepared using traditional routes.[22] Therefore, a mild and an alternative route to functionalize FWNTs is adopted in this study. The approach is conceptualized on the basis of our foray into the CNT chemistry using "direct" Friedel−Crafts acylation technique, which has superior operational simplicity.[10,14,19−21,23−27] This strategy was previously shown to be a less destructive and/or nondestructive reaction condition for the efficient dispersion and functionalization of carbon nanomaterials. As a result, CNT damage from severe chemical treatments including oxidation and sonication can be avoided to a larger extent. A schematic cartoon of the experimental procedure governing the grafting of EBA onto the FWNT is presented in Figure 1.

Also depicted in Figure 1 are the digital photographs of reaction flask, EBA-*f*-FWNT dispersed in water, and the prepared thin films at various stages. The shiny reaction mixture was a strong indication that FWNT bundles were uniformly dispersed in the reaction mixture (Figure 1b). The reaction mixture was poured into deionized water. EBA-*f*-FWNT was stably dispersed for a week (Figure 1c). Interestingly, the dispersion emitted strong green light under room light, implying that the EBA moieties were indeed uniformly functionalized and dispersed well (Figure 1d). High-quality and flexible free-standing thin film could simply be prepared from the solution by suction filtration (Figure 1e). Unlike reported acid-treated CNT thin films,[28] the paper-like free-standing thin film we prepared could be rolled up, twisted, bent over easily, and even folded without any drastic cracking on the films (Figure 1f). It should be noted, however, that too much pressure exerted on the films leads to a few cracks on the bent region alone. Nevertheless, this flexible transition could be a significant advancement for the CNT thin film studies for various applications. It is noteworthy that FWNTs are easier to exfoliate than any other forms of CNTs, making them akin to easy processability. The diameter dimension of the films shown in Figure 1 is 3.3 cm, but they could also potentially be scaled up for large-area flexible electronics applications, namely, by spraying techniques or other methods. Investigating the structural integrity and the conductive property of the thin film after carbonization was an interesting task. Hence, the thin film was cut in half and carbonized at 600 °C for 2 h in nitrogen atmosphere in a heating furnace. It was believed that, after such a carbonization process, most of the attached EBA moieties get burnt and the surface of the film should deteriorate. Surprisingly, however, we found that the film itself retained its original shape and external texture morphology as clearly seen (Figure 1g) and still could be bent and twisted to certain extent, which indicated the robustness of the prepared thin film.

FT-IR and Raman spectroscopies were employed to characterize the initial changes in surface functionalities formed after processing. FT-IR spectroscopy, often a powerful tool, was used to elucidate the covalent attachment between the FWNTs and EBA. Shown in Figure 2 are the spectra obtained for the pristine FWNTs and the functionalized thin films. A very distinct difference between the pristine and the functionalized thin films can be observed. Figure 2a shows the characteristic vibration bands of FWNTs, wherein an absorption peak at 1600 cm$^{-1}$ can be attributed to the vibration of the carbon skeleton. Slight traces of sp$^2$-C−H and sp$^3$-C−H stretching bands due to the intrinsic structural defects present in the neat FWNTs are also visible near 2920 cm$^{-1}$. On the other hand, however, the pronounced increase in intensity of this peak in the functionalized films is direct evidence that the substitution of EBA moieties has taken place due to the Friedel−Crafts acylation strategy, as seen in Figure 2a. Additionally, the
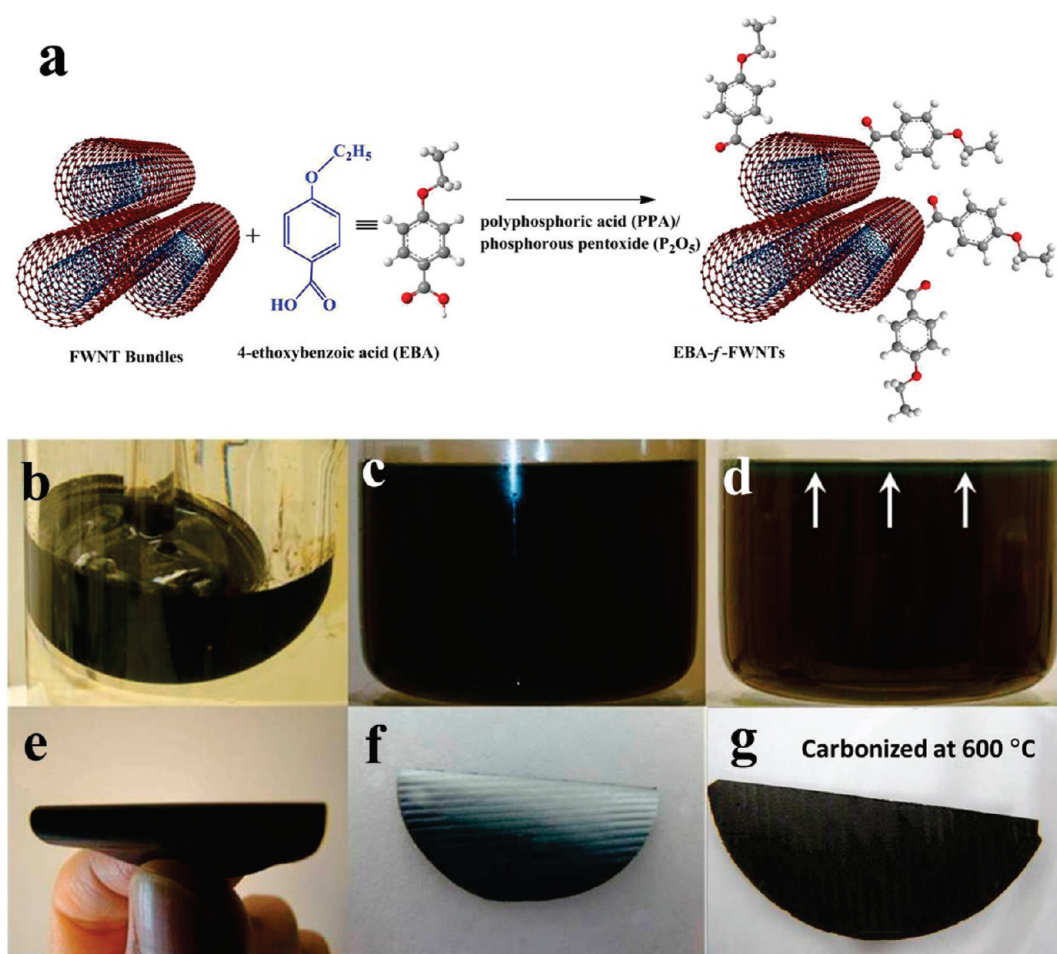
**Figure 1.** Schematic cartoon depicting the functionalization procedure of FWNTs with EBA (a). Digital photographs: (b) reaction flask; (c) EBA-*f*-FWNT dispersed in water without room light; (d) with top room light on, showing strong green emission on the surface of solution; (e) prepared EBA-*f*-FWNT thin film with diameter of *ca.* 3.3 cm, showing the flexibility; (f) 180° folded EBA-*f*-FWNT thin film; (g) carbonized EBA-*f*-FWNT thin film at 600 °C for 2 h.

presence of a strong band at around 1719 cm$^{-1}$ obtained from the thin film shows the −C=O stretching modes of the carbonyl linkages between the FWNTs and the EBA moieties, which clearly suggests and supports the fact that the reaction was indeed covalent in nature. This also indicates that the desired exchange had occurred between the FWNTs and the carboxyl groups present on the EBA moieties. In the case of the carbonized film, most of the characteristic peaks attributed to the thin films could be observed, which suggests that, even after carbonization, a few percent of the functional groups attached to FWNTs remain intact.

As a well-known fact, Raman spectroscopy can indicate the functionalization type and also the surface properties to an extent. Shown in Figure 2b is the Raman spectrum for the pristine and the FWNT thin film. The D band found near 1300 cm$^{-1}$ is generally used to evaluate the defect density present in the tubular wall structure. Interestingly, as seen from the Figure 2b, the relative intensity of the D band of the FWNT thin film slightly decreased with respect to the neat FWNTs. On the other hand, however, when

normalized, the relative intensity in the 2D band, which implies the quality of graphitic structure,[29] sharply increased for the carbonized samples. The spectra clearly indicate that the covalent functionalization of FWNTs in a mild PPA/P$_2$O$_5$ medium is indeed a less and/or nondestructive condition.

Electron microscopic observations were performed primarily to visualize and investigate the structural aspects and detailed morphologies of the prepared EBA-*f*-FWNT. In all cases, a homogeneous network of EBA-*f*-FWNT is observed. FE-SEM and the corresponding cross-section images of the thin films are depicted in Figure 3a−c. From SEM observations, it was found that the diameters of the EBA-*f*-FWNT bundles (Figure 3b) increased dramatically after functionalization, which clearly indicates that the EBA groups were well coated on the FWNT sidewalls. In addition, the functionalized tubes are highly tangled with each other, forming a network (Figure 3b). These surface images visually support the suggestion that EBA moieties were indeed covalently linked to the surface of FWNTs. The sustainability of the tube structures to such
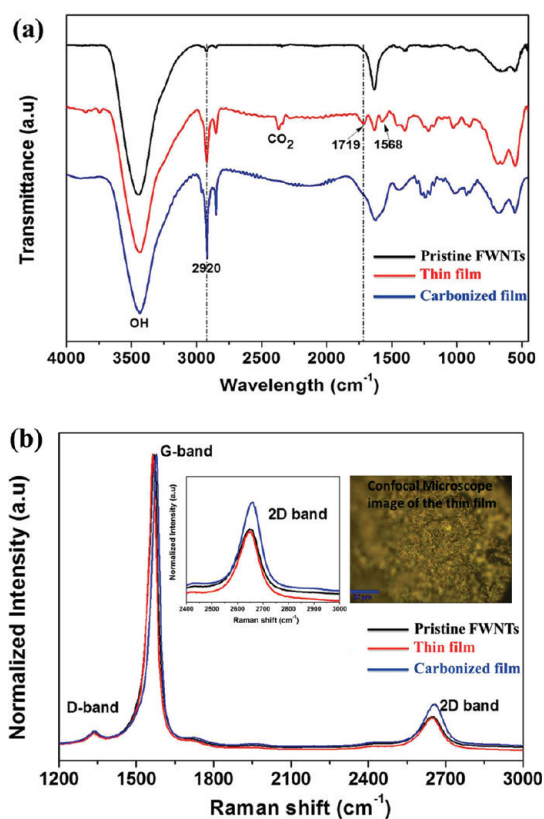
**Figure 2.** (a) FT-IR spectra and (b) normalized Raman spectra of pristine FWNTs and before and after carbonized EBA-*f*-FWNT thin films. Insets in (b) show short scan image depicting increased intensity in the 2D band (left) and the confocal microscope image of the EBA-*f*-FWNT thin film surface (right).

a functionalization reaction is also proven here. Observation of cross sections of complex materials provides crucial information about the layered structures, the film thicknesses of reaction layers, and the existence of voids and so on. Cross-section images of the EBA-*f*-FWNT thin films are depicted in the Figure 3c for better understanding of the layer structures. Measurements from the cross-sectional SEM image of the film suggest that the thickness of film is approximately 18 $\mu$m. Clearly, the image at high magnification (Figure S1 in the Supporting Information) also verified the dense and uniform packing of the tubes throughout the film, which was notably achieved without the addition of a chemical binder or a cross-linking agent.

For clarity, the corresponding high-resolution TEM images of the pristine FWNTs and the prepared thin films at different magnifications are shown in Figure 3d–f. Similar to the FE-SEM images, the TEM images reveal FWNTs with spaghetti-like morphology (Figure 3d). While the pristine FWNT bundle has a clean and smooth surface (Figure 3e), close scrutiny of the TEM images reveals that the resulting EBA-*f*-FWNT has coaxially tubular structures where its walls were well-encapsulated with the EBA layers (Figure 3f). Additionally, the diameter of the functionalized FWNTs was found to be around 5 nm with an average of 4–5 graphitic layers as marked with arrows in

the image (Figure 3f). The formation of a core–shell structure was also noticed, with the FWNTs being the cores, encapsulated by EBA moieties. The core–shell structures well indicate the covalent links between the EBA moieties and the FWNTs. In most areas of the holey carbon grid, the suspension of the functionalized FWNTs was uniform without any visible agglomerations, and these core–shell structures were present uniformly throughout the sample (Figure S2 in the Supporting Information). Furthermore, it should also be noted that the TEM studies can shed direct light on the quality of the FWNT dispersion in the EBA-*f*-FWNT films. Notably, from the TEM images, it is clear that the EBA-*f*-FWNTs exhibited good dispersion in water. Clearly, the direct Friedel–Crafts acylation technique has suggested and supported the fact that the functionalization procedure does not destroy the tubes but preserves the graphitic lattice, hence preserving the intrinsic properties of the FWNTs.

The content of the EBA moieties that were attached onto the FWNT surface in the EBA-*f*-FWNT thin films and the comparison of mass losses of pristine FWNTs upon heating in air and nitrogen atmosphere were determined thermogravimetrically and are shown in Figure 4.

Neat FWNTs were more stable in nitrogen atmosphere and did not show any dramatic decomposition in the temperature range of 50–500 °C. Upon functionalization, stepwise weight loss patterns were found for the thin films in air. The first stage weight loss occurring from 250 to 500 °C should be due to the thermal decomposition of aliphatic groups (Figure 4a). The second stage rapid weight loss ranging from 450 to 650 °C can be attributed to the oxidative degradation of the aromatic benzoyl units (Figure 4a). The degree of functionalization from the gradual mass loss of the EBA-*f*-FWNT suggests that around 33 wt % has been functionalized to the tubes. As a result, it could be concluded that the thermal stability of the hybrid composite appears to be better than the pristine FWNT and it starts oxidation at a relatively higher temperature.

In a general point of view, it is believed that extensive oxidation can shorten the CNTs and thereby impair its intrinsic mechanical properties and negatively affect mechanical properties of resulting CNT reinforced composites. The stress–strain curve for the EBA-*f*-FWNT thin film is shown in Figure 5. In this case, at least six strips were measured and the first one was broken at a grip, as shown in the inset image. Thus, the average mean values are taken into account from the rest of the five tests. It is understood that the composite films acquired a more pronounced improvement in terms of mechanical properties and significant increase in tensile properties. Furthermore, experimental results for the composite films exhibit higher values of tensile stress and elongation at break approaching 80 MPa. These results indicate that the mechanical properties of the EBA-*f*-FWNT films are substantially superior to those of neat CNTs or even single-walled CNTs reported elsewhere.[30]
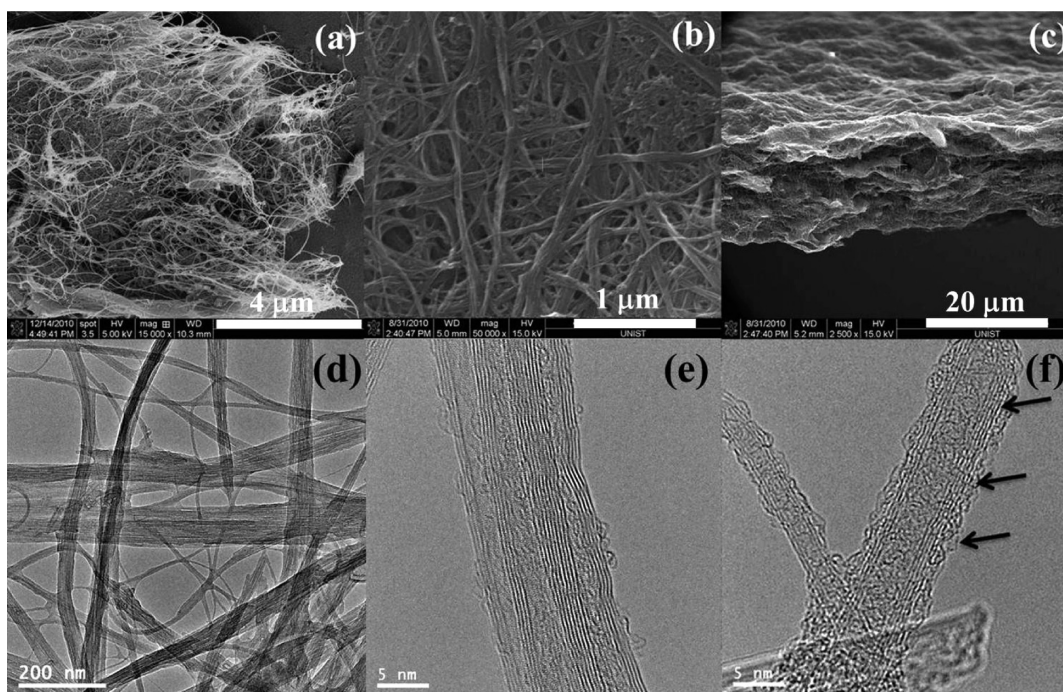
**Figure 3.** FE-SEM images: (a) pristine FWNTs; (b) the surface of EBA-*f*-FWNT thin film; (c) cross section of the thin film. HR-TEM images: (d,e) pristine FWNTs at different magnifications; (f) EBA-*f*-FWNT.
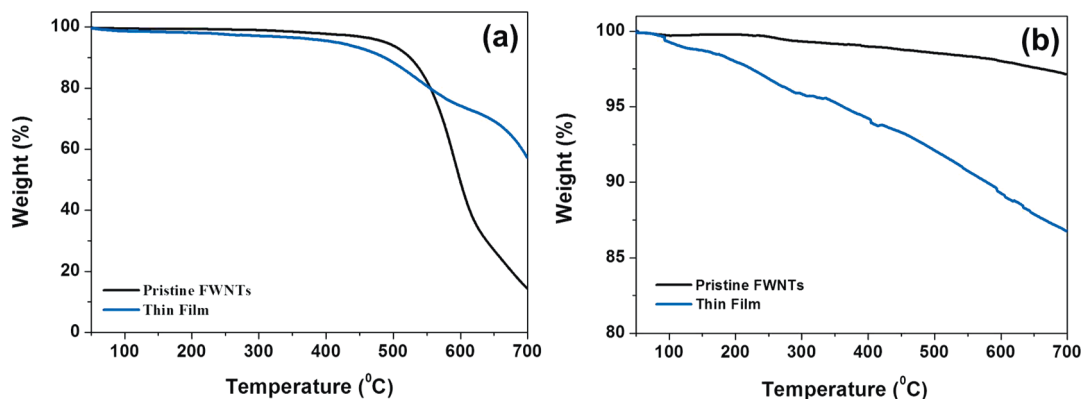


**Figure 4.** TGA thermograms of pristine FWNTs and EBA-*f*-FWNT thin film: (a) in air; (b) in nitrogen.

The electrical conductivities of the two types of composites prepared were measured by a programmable standard four-point probe method under laboratory conditions. The average electrical conductivities of the as-prepared thin films were found to be 29 400 S m$^{-1}$, surprisingly even better than a transparent carbon film electrode reported recently with a value of 206 S cm$^{-1}$.[31] Compared to the reported polymer–nanotube thin films[32] or even comparing with doped MWNTs as reported,[33] our results by far stand the best for such a simple strategy. The results indicate that the formation of a conducting network in the EBA-*f*-FWNT thin films results in improved electrical properties. Interesting to note is that even after carbonizing the thin film at 600 °C for 2 h, the sample shows an electrical conductivity in the range of 14 940 S m$^{-1}$.
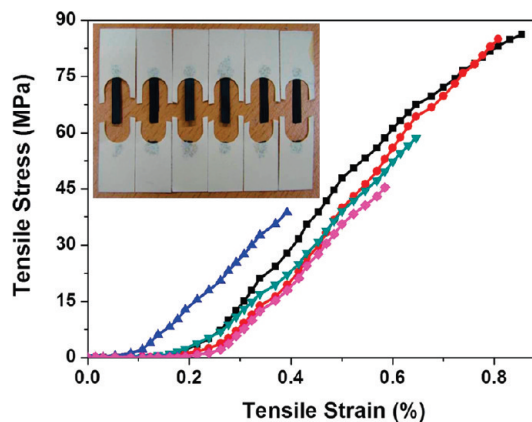


**Figure 5.** Tensile stress−strain curves for five different measurements of the EBA-*f*-FWNT thin film. Inset image shows the tensile test specimens.
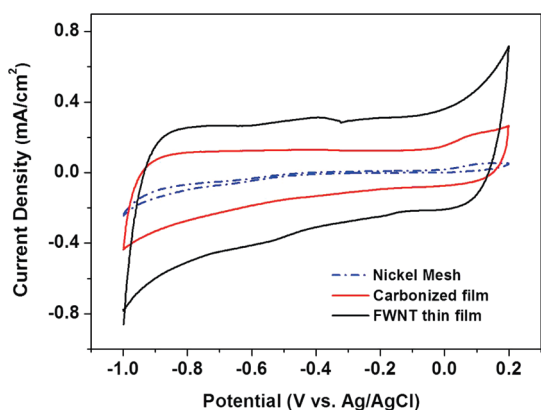
**Figure 6.** Cyclic voltammograms (CV) of nickel mesh, before and after carbonized EBA-*f*-FWNT thin film electrodes in 0.1 M aqueous KOH solution with a sweep rate of 10 mV/s.

Cyclic voltammetry (CV) experiments were done to evaluate the electrochemical performance of functionalized FWNT thin films. In our work, the films itself were used as the working electrode. For this, special nickel mesh holders were designed to hold the thin film in a standard three-electrode electrochemical cell. Figure 6 shows the CV curves of samples in 0.1 M aqueous KOH solution. In order to omit the current obtained from nickel, the bare nickel mesh was run as a standard before the thin films were used as electrodes. The measured CV curves show a quite rectangular shape. The voltammograms were used to calculate the specific capacitance of the thin film electrodes. The specific capacitance using the CV curves was reported by integrating over the full CV curve using the in-built program to determine the average area value for one cycle. The calculated specific capacitance

was found to be 133 F/g for the thin film electrode and ~75 F/g for the carbonized film electrode.

This kind of rectangular shaped CV curve coupled with such a high specific capacitance is another indication that these kinds of films are thus very attractive for capacitor applications. It is quite noteworthy that, even for first 100 cycles for both the thin film and the carbonized film electrodes, the CV curves were very stable and show profoundly high current densities (see Supporting Information, Figures S3 and S4). These results suggest that the EBA-*f*-FWNT films could have superior electrochemical behavior and could be very attractive for several applications including supercapacitors.

## CONCLUSION

Highly conducting and flexible free-standing thin films were prepared by functionalizing FWNTs with 4-ethoxybenzoic acid (EBA) in a less destructive PPA/$P_2O_5$ *via* a direct Friedel−Crafts acylation reaction. On the basis of characterization results, EBA was well-coated on FWNTs with core−shell structures forming highly conductive networks. Electrical conductivity of these CNT-based assemblies showed values nearing as high as 29 400 S m$^{-1}$. Furthermore, these highly flexible films depicted enhanced mechanical properties with stress−strain values for elongation at break nearly 80 MPa. This study demonstrates the ability of the simple preparation technique to produce highly flexible and conductive nanotube-based thin films which renders the material suitable for creating miniaturized devices and flexible electrodes, thus opening new possibilities for their prospective technological applications.

## METHODS

**Materials.** All reagents were purchased form Aldrich Chemicals Inc., USA, and were used as received. Few-walled carbon nanotubes (FWNT with diameter of 3−8 nm and length of ~20 $\mu$m, metallic impurities <4 wt %) were obtained from Carbon Nanotechnologies Inc. (CNI), Houston, TX.

**Instrumentations.** The morphologies of the thin films were analyzed by field emission scanning electron microscopy (FE-SEM), performed on a LEO 1530FE and FEI NanoSem 200. For the SEM cross-section images, the FWNT thin film samples were cracked by sequential dipping in liquid nitrogen and then affixed to SEM mounts with carbon tape. For the microscopic imaging with high-resolution transmission electron microscopy (HR-TEM), the thin films were embedded in epoxy resin and were cured at 70 °C for 6 h. This film was then sliced into thin cross sections using a microtome (Model-RMC Powertome PC by Boeckeler) equipped with a diamond blade. The sliced cross sections were floated onto carbon-coated copper TEM grids and analyzed using a JEOL JEM 2100 TEM at an accelerating voltage of 200 kV. The initial changes in the surface chemical bonding and the grafting behavior of the EBA moieties onto the FWNT surface were recorded by Fourier transformed infrared spectrophotometry (FT-IR, Perkin-Elmer s100, USA), in the frequency range of 4000−450 cm$^{-1}$. The content of the EBA moieties in the hybrid thin films was determined thermogravimetrically using TGA (TA Instruments, USA). The sheet resistance and the electrical conductivity of the as-prepared thin films

were determined *via* a standard four-point probe method using Advanced Instrument Technology (AIT) CMT-SR1000N with Jandel Engineering probe at ambient temperature. Appropriate correction factors were used to calculate the conductivity values, which were the averages of 10 measurements of the same film. The mechanical properties of the composite films were investigated with a DMA tensile tester from TA Instruments, USA.

For the electrochemical measurements, cyclic voltammetry (CV) was carried out using a VersaSTAT3 AMETEK Model (Princeton Applied Research) potentiostat/galvanostat employing a standard three-electrode electrochemical cell, which consisted of the functionalized FWNT thin film as the working electrode, an Ag/AgCl as the reference electrode, and platinum gauze as the counter electrode. Experiments were carried out at room temperature in 0.1 M aqueous KOH solution as the electrolyte with a nickel mesh holder specially designed in-house to hold CNT thin films. All potentials are reported relative to an Ag/AgCl (saturated KCl) reference electrode recorded at a scan rate of 10 mV s$^{-1}$. The potential window for cycling was confined between −1.0 and 0.2 V so as to omit the extra current generated by nickel mesh.

**Functionalization and Film Formation of FWNTs.** Into a resin flask equipped with a high torque mechanical stirrer, nitrogen inlet, and outlet, 4-ethoxybenzoic acid (0.3 g, 1.8 mmol), FWNT (0.2 g), PPA (20.0 g, 83% $P_2O_5$ assay), and $P_2O_5$ (5.0 g) were placed. The flask was immersed in an oil bath, gently heated to 100 °C, and maintained at that temperature with stirring for 24 h under nitrogen atmosphere. It was then heated to 130 °C and stirred

for 24 h. The dark homogeneous mixture was poured into water. The resulting 4-ethylbenzoyl-functionalized FWNT (EBA-*f*-FWNT) was uniformly dispersed in water. The dispersed solution emitted deep green color under room light (see digital photo in Figure 1d). The solution was stable for a week when left standing at ambient conditions. EBA-*f*-FWNT thin films were fabricated by suction filtration of the solution. The films formed on membranes were dried in air and delaminated from the membrane. To prevent the formation of wrinkles, the films were sandwiched in waxed weighing papers and 500 g weight was placed on them for a day. The films were transferred into extraction thimble and Soxhlet extracted with distilled water to completely remove reaction medium for 3 days and then with methanol to get rid of other possible organic impurities for 3 days, and finally dried at 100 °C under reduced pressure for 24 h to yield dark black thin films.

*Supporting Information Available:* Higher magnification FE-SEM image, lower magnification TEM and CV curves for 100 cycles. This material is available free of charge *via* the Internet at http://pubs.acs.org.

## REFERENCES AND NOTES

1. Karousis, N.; Tagmatarchis, N.; Tasis, D. Current Progress on the Chemical Modification of Carbon Nanotubes. *Chem. Rev.* **2010,** *110*, 5366–5397.
2. Yürüm, Y.; Taralp, A.; Veziroglu, T. N. Storage of Hydrogen in Nanostructured Carbon Materials. *Int. J. Hydrogen Energy* **2009,** *34*, 3784–3798.
3. Kaskhedikar, N. A.; Maier, J. Lithium Storage in Carbon Nanostructures. *Adv. Mater.* **2009,** *21*, 2664–2680.
4. Zhang, T.; Mubeen, S.; Myung, N. V.; Deshusses, M. A. Recent Progress in Carbon Nanotube-Based Gas Sensors. *Nanotechnology* **2008,** *19*, 332001.
5. Cao, Q.; Rogers, J. A. Ultrathin Films of Single-Walled Carbon Nanotubes for Electronics and Sensors: A Review of Fundamental and Applied Aspects. *Adv. Mater.* **2009,** *21*, 29–53.
6. Park, Y. D.; Lim, J. A.; Jang, Y.; Hwang, M.; Lee, H. S.; Lee, D. H.; Lee, H.-J.; Baek, J.-B.; Cho, K. Enhancement of the Field-Effect Mobility of Poly(3-hexylthiophene)/Functionalized Carbon Nanotube Hybrid Transistors. *Org. Electron.* **2008,** *9*, 317–322.
7. Hatton, R. A.; Miller, A. J.; Silva, S. R. P. Carbon Nanotubes: A Multi-functional Material for Organic Optoelectronics. *J. Mater. Chem.* **2008,** *18*, 1183–1192.
8. Avouris, P.; Freitag, M.; Perebeinos, V. Carbon-Nanotube Photonics and Optoelectronics. *Nat. Photonics* **2008,** *2*, 341–350.
9. Scardaci, V.; Coull, R.; Coleman, J. N. Very Thin Transparent, Conductive Carbon Nanotube Films on Flexible Substrates. *Appl. Phys. Lett.* **2010,** *97*, 023114.
10. Kang, J. Y.; Eo, S. M.; Jeon, I. Y.; Choi, Y. S.; Tan, L. S.; Baek, J.-B. Multifunctional Poly(2,5-benzimidazole)/Carbon Nanotube Composite Films. *J. Polym. Sci., Part A: Polym. Chem.* **2010,** *48*, 1067–1078.
11. Hou, Y.; Tang, J.; Zhang, H.; Qian, C.; Feng, Y.; Liu, J. Functionalized Few-Walled Carbon Nanotubes for Mechanical Reinforcement of Polymeric Composites. *ACS Nano* **2009,** *3*, 1057–1062.
12. Qian, C.; Qi, H.; Liu, J. Effect of Tungsten on the Purification of Few-Walled Carbon Nanotubes Synthesized by Thermal Chemical Vapor Deposition Methods. *J. Phys. Chem. C* **2006,** *111*, 131–133.
13. Qi, H.; Qian, C.; Liu, J. Synthesis of High-Purity Few-Walled Carbon Nanotubes from Ethanol/Methanol Mixture. *Chem. Mater.* **2006,** *18*, 5691–5695.
14. Jeon, I.-Y.; Choi, J. I.; Lee, S. G.; Chae, H. G.; Jang, S. S.; Kumar, S.; Baek, J.-B. Sponge Behaviors of Functionalized Few-Walled Carbon Nanotubes. *J. Phys. Chem. C* **2010,** *114*, 14868–14875.
15. Dyke, C. A.; Tour, J. M. Covalent Functionalization of Single-Walled Carbon Nanotubes for Materials Applications. *J. Phys. Chem. A* **2004,** *108*, 11151–11159.
16. Sun, Y.-P.; Fu, K.; Lin, Y.; Huang, W. Functionalized Carbon Nanotubes: Properties and Applications. *Acc. Chem. Res.* **2002,** *35*, 1096–1104.
17. Kumar, N. A.; Bund, A.; Cho, B. G.; Lim, K. T.; Jeong, Y. T. Novel Amino-Acid-Based Polymer/Multi-walled Carbon Nanotube Bio-nanocomposites: Highly Water Dispersible Carbon Nanotubes Decorated with Gold Nanoparticles. *Nanotechnology* **2009,** *20*, 225608.
18. Kumar, N. A.; Jeong, Y. T. Fabrication of Conducting Polyaniline—Multiwalled Carbon Nanotube Nanocomposites and Their Use as Templates for Loading Gold Nanoparticles. *Polym. Int.* **2010,** *59*, 1367–1374.
19. Lee, H. J.; Han, S. W.; Kwon, Y. D.; Tan, L. S.; Baek, J.-B. Functionalization of Multi-walled Carbon Nanotubes with Various 4-Substituted Benzoic Acids in Mild Polyphosphoric Acid/Phosphorous Pentoxide. *Carbon* **2008,** *46*, 1850–1859.
20. Lee, H. J.; Oh, S. J.; Choi, J. Y.; Kim, J. W.; Han, J.; Tan, L. S.; Baek, J.-B. *In Situ* Synthesis of Poly(ethylene terephthalate) (PET) in Ethylene Glycol Containing Terephthalic Acid and Functionalized Multiwalled Carbon Nanotubes (MWNTs) as an Approach to MWNT/PET Nanocomposites. *Chem. Mater.* **2005,** *17*, 5057–5064.
21. Oh, S. J.; Lee, H. J.; Keum, D. K.; Lee, S. W.; Wang, D. H.; Park, S. Y.; Tan, L. S.; Baek, J.-B. Multiwalled Carbon Nanotubes and Nanofibers Grafted with Polyetherketones in Mild and Viscous Polymeric Acid. *Polymer* **2006,** *47*, 1132–1140.
22. Wepasnick, K. A.; Smith, B. A.; Schrote, K. E.; Wilson, H. K.; Diegelmann, S. R.; Fairbrother, D. H. Surface and Structural Characterization of Multi-walled Carbon Nanotubes Following Different Oxidative Treatments. *Carbon* **2011,** *49*, 24–36.
23. Baek, J.-B.; Lyons, C. B.; Tan, L.-S. Grafting of Vapor-Grown Carbon Nanofibers *via* In-Situ Polycondensation of 3-Phenoxybenzoic Acid in Poly(phosphoric acid). *Macromolecules* **2004,** *37*, 8278–8285.
24. Choi, E. K.; Jeon, I. Y.; Bae, S. Y.; Lee, H. J.; Shin, H. S.; Dai, L.; Baek, J.-B. High-Yield Exfoliation of Three-Dimensional Graphite into Two-Dimensional Graphene-like Sheets. *Chem. Commun.* **2010,** *46*, 6320–6322.
25. Jeon, I. Y.; Kang, S. W.; Loon-Seng, T. A. N.; Baek, J.-B. Grafting of Polyaniline onto the Surface of 4-Aminobenzoyl-Functionalized Multiwalled Carbon Nanotube and Its Electrochemical Properties. *J. Polym. Sci., Part A: Polym. Chem.* **2010,** *48*, 3103–3112.
26. Jeon, I. Y.; Loon-Seng, T. A. N.; Baek, J.-B. Synthesis and Electrical Properties of Polyaniline/Polyaniline Grafted Multiwalled Carbon Nanotube Mixture *via* In Situ Static Interfacial Polymerization. *J. Polym. Sci., Part A: Polym. Chem.* **2010,** *48*, 1962–1972.
27. Jeon, I.-Y.; Lee, H.-J.; Choi, Y. S.; Tan, L.-S.; Baek, J.-B. Semimetallic Transport in Nanocomposites Derived from Grafting of Linear and Hyperbranched Poly-(phenylene sulfide)s onto the Surface of Functionalized Multi-walled Carbon Nanotubes. *Macromolecules* **2008,** *41*, 7423–7432.
28. Spitalský, Z.; Aggelopoulos, C.; Tsoukleri, G.; Tsakiroglou, C.; Parthenios, J.; Georga, S.; Krontiras, C.; Tasis, D.; Papagelis, K.; Galiotis, C. The Effect of Oxidation Treatment on the Properties of Multi-walled Carbon Nanotube Thin Films> *Mater. Sci. Eng., B* **2009,** *165*, 135–138.
29. Ferrari, A. C.; Meyer, J. C.; Scardaci, V.; Casiraghi, C.; Mazzeri, M.; Mauri, F.; Piscanec, S.; Jiang, D.; Novoselov, K. S.; Roth, S.; *et al.* Raman Spectrum of Graphene and Graphene Layers. *Phys. Rev. Lett.* **2006,** *97*, 187401.
30. Zhang, X.; Sreekumar, T. V.; Liu, T.; Kumar, S. Properties and Structure of Nitric Acid Oxidized Single Wall Carbon Nanotube Films. *J. Phys. Chem. B* **2004,** *108*, 16435–16440.

31. Wang, X.; Zhi, L.; Tsao, N.; Tomović, Ž.; Li, J.; Müllen, K. Transparent Carbon Films as Electrodes in Organic Solar Cells. *Angew. Chem., Int. Ed.* **2008,** *47*, 2990–2992.

32. Lahiff, E.; Leahy, R.; Coleman, J. N.; Blau, W. J. Physical Properties of Novel Free-Standing Polymer−Nanotube Thin Films. *Carbon* **2006,** *44*, 1525–1529.

33. Zhou, C.; Wang, S.; Zhuang, Q.; Han, Z. Enhanced Conductivity in Polybenzoxazoles Doped with Carboxylated Multi-walled Carbon Nanotubes. *Carbon* **2008,** *46*, 1232–1240.